

Fig. S1. CH₄ consumption by Lake Stechlin sediment incubated at 4°C.

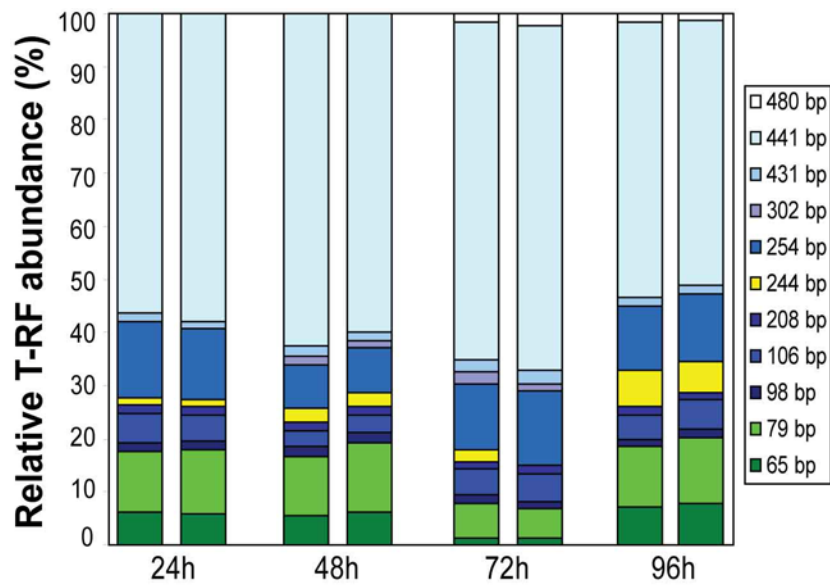


Fig. S2. T-RFLP profiles of *pmoA* genes recovered from the sediment during the SIP time-course incubations. At each time point, the profiles from the $^{12}\text{CH}_4$ incubation (left bar) and $^{13}\text{CH}_4$ incubation (right bar) are shown.

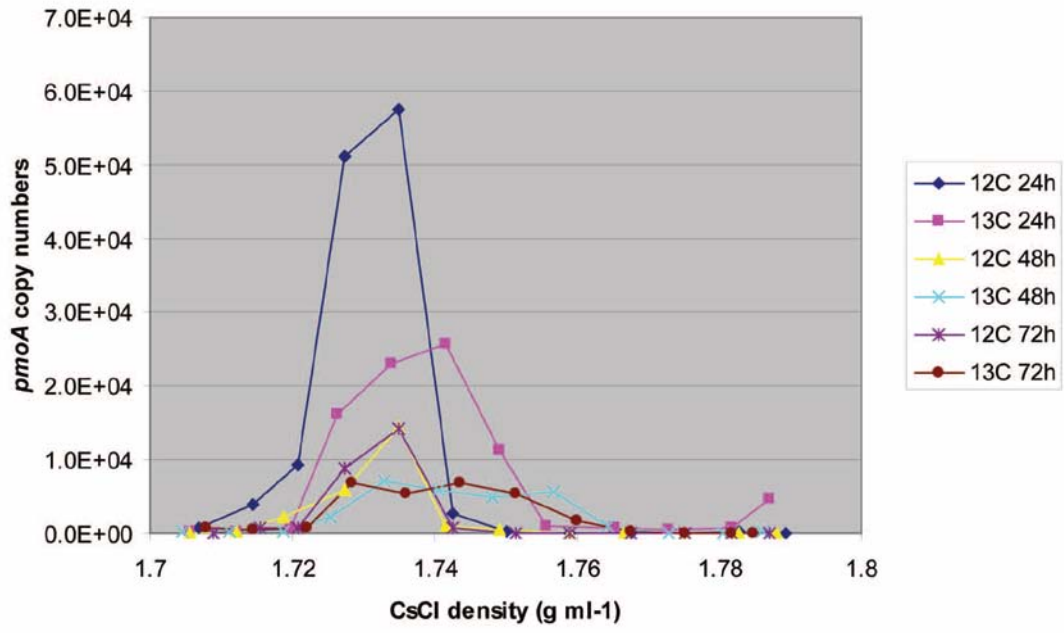


Fig. S3. Absolute values of *pmoA* gene copies per CsCl gradient fraction.

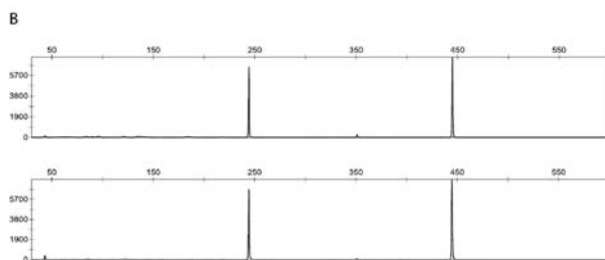
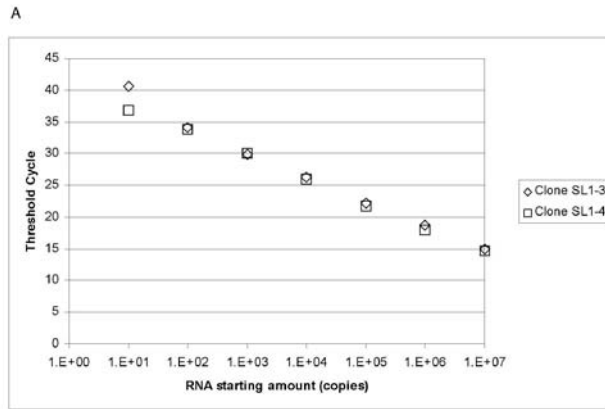


Fig. S4. Quantitative PCR (A) test for bias against reverse transcription of type II *pmoA* mRNA. RNA was produced by *in vitro* transcription of a type II *pmoA* clone (SL1-3) and type Ia clone (SL1-4). 5×10^8 RNA copies of each clone were reverse transcribed. The cDNA was serially diluted and used as templates in qPCR. The threshold cycles were the same for each sequence, indicating that equivalent amounts of cDNA was generated from both RNA sequences. In (B) we performed a similar test using T-RFLP by mixing equivalent amounts of the *in vitro* transcripts (top panel) and performing reverse transcription followed by PCR and T-RFLP; as a comparison, the two sequences types were mixed after the reverse transcription (lower panel). Both showed nearly equivalent amounts of the sequence types (SL1-3 T-RF is 244 bp and SL1-4 T-RF is 441 bp) and identical results if the reverse transcription was performed as a mixture or separately.

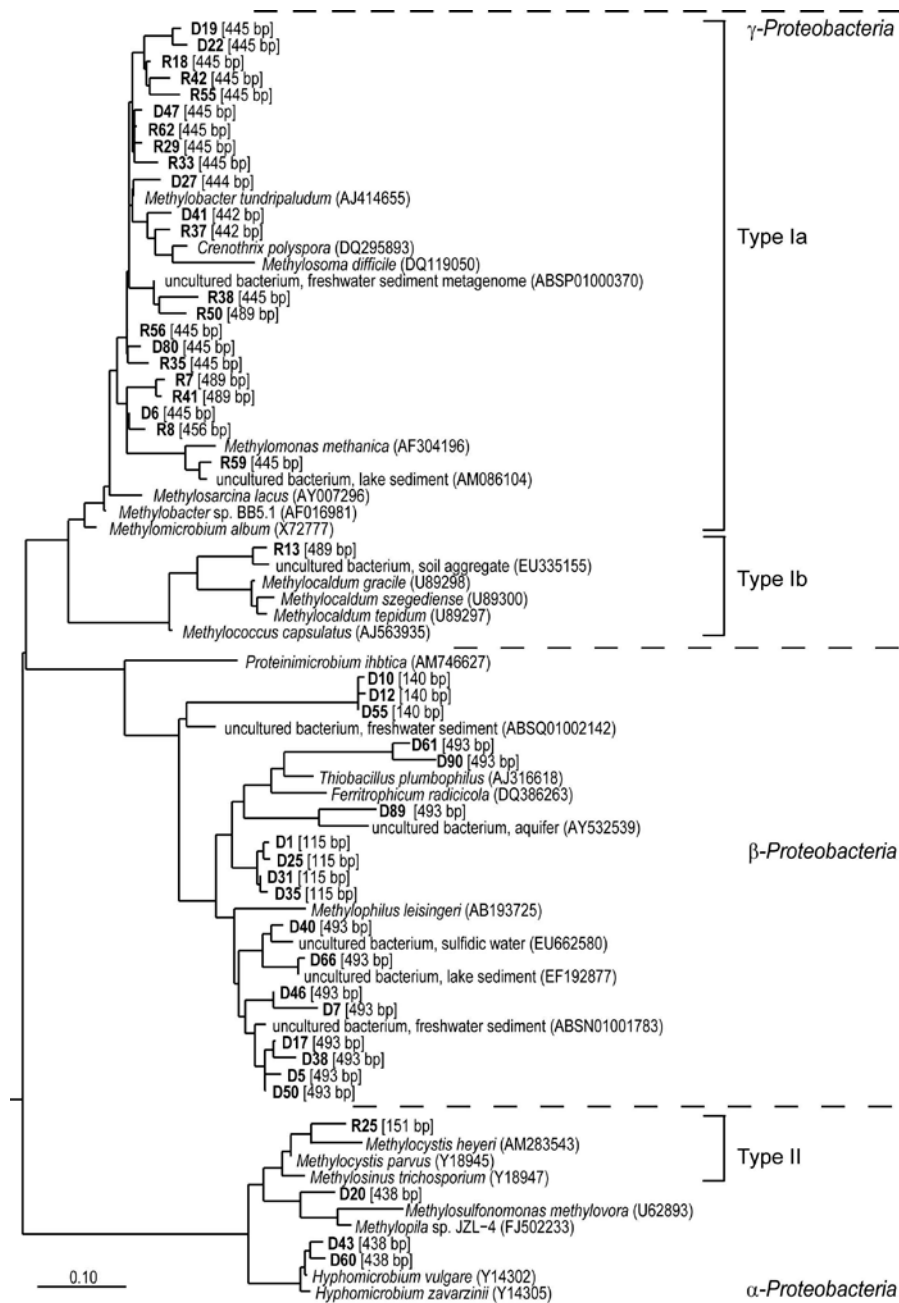


Fig. S5. Maximum-likelihood phylogenetic tree of representative 16S rRNA sequences obtained from the heavy fraction of SIP gradients. The clone names are indicated in boldtype and the observed T-RF size for the clones is indicated in square brackets. The clone names beginning with ‘R’ originate from RNA-SIP gradients and those with ‘D’ from DNA-SIP gradients. Representative sequences from various bacterial phyla were used as outgroup (not shown). The Genbank accession numbers of reference sequences are shown in brackets.

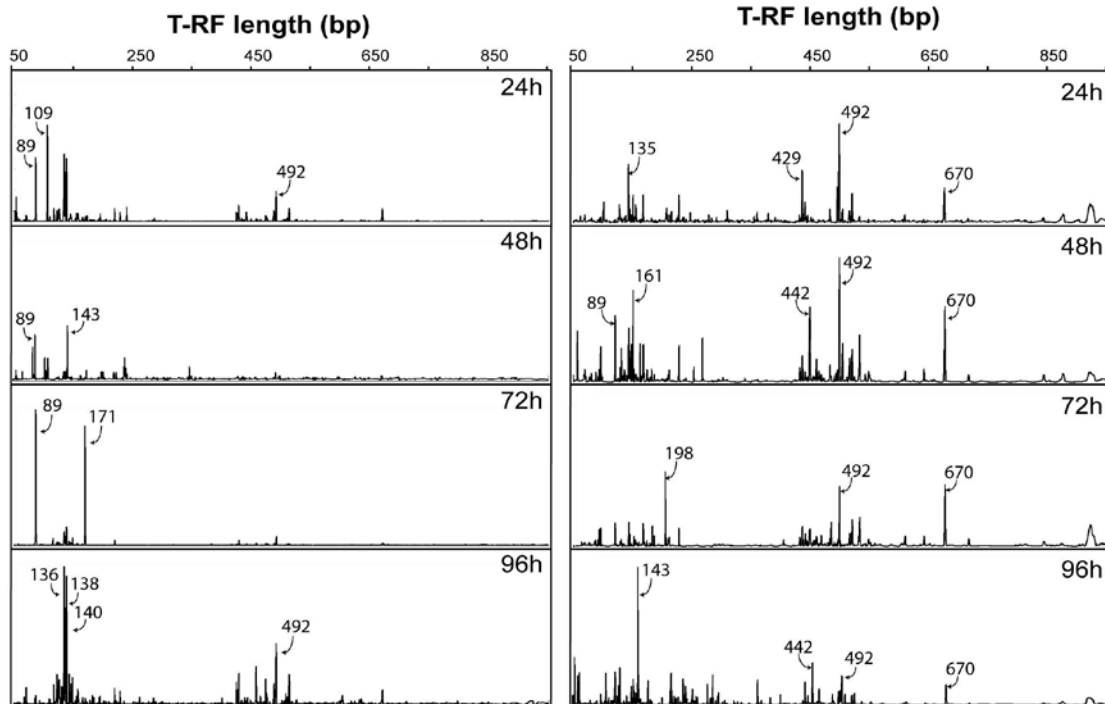
A. $^{12}\text{CH}_4$, heavy fraction, DNA**B. $^{12}\text{CH}_4$, heavy fraction, RNA**

Fig. S6. 16S rRNA T-RFLP profiles in the heavy fractions of gradients from $^{12}\text{CH}_4$ incubated control samples. DNA-SIP (A) and RNA-SIP (B) gradients are shown. The characteristic T-RFs associated with the heavy fractions from $^{13}\text{CH}_4$ incubations (Figures 5 & 6) are not present, indicating that those T-RFs are indeed from labelled nucleic acids.

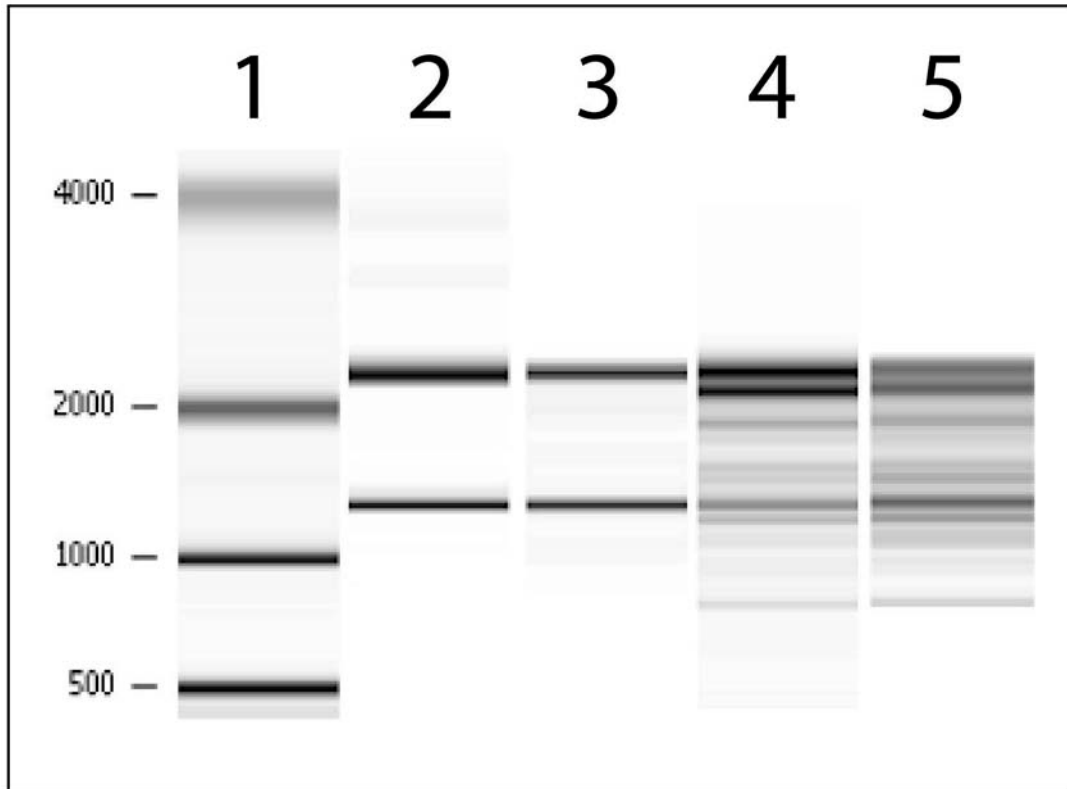


Fig. S7. *E. coli* RNA analysis with a Bioanalyzer™. The illustration is a simulated gel image produced by the accompanying software. Lanes: 1, RNA size standard; 2, total RNA uncentrifuged; 3, total RNA centrifuged and recovered from the CsTFA gradient; 4, enriched mRNA uncentrifuged; 5, enriched mRNA centrifuged and recovered from CsTFA gradient.

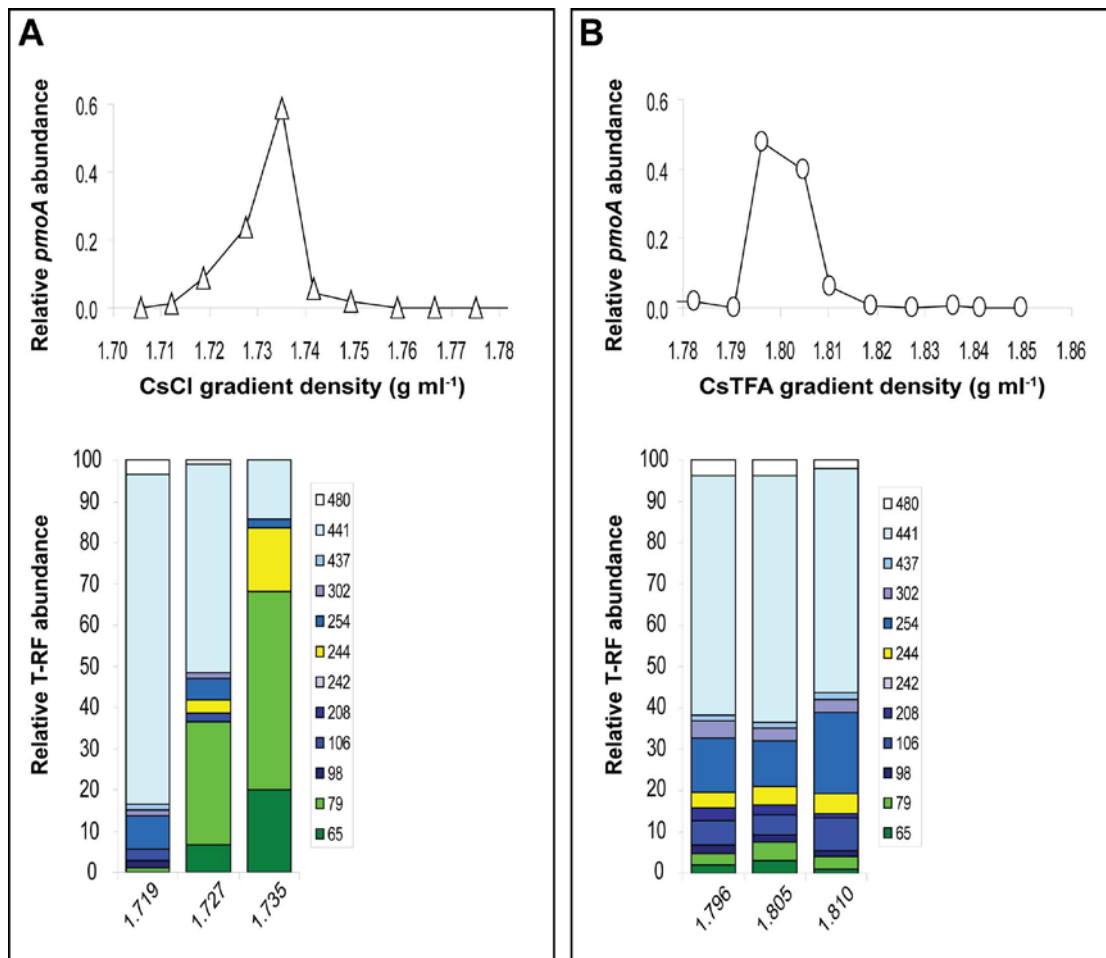


Fig. S8. Investigation of *pmoA* distribution in caesium gradients containing Lake Stechlin DNA (A) or mRNA (B). The uppermost plots show the relative abundance of *pmoA* in each of the gradient fractions as determined by qPCR and RT-qPCR, respectively. The lower plots show the *pmoA* T-RFLP data for the gradient fractions containing *pmoA* genes (A) and transcripts (B). The type Ia *pmoA* sequences (blue T-RFs) have lower G+C contents than the type Ib (green) and type II (yellow), which was reflected in the distribution of DNA (A), but not RNA (B). The results show a strong effect of G+C content on the distribution of *pmoA* genes in CsCl gradients, but no such effect of the *pmoA* transcripts in CsTFA gradients.